RAPID COMMUNICATION

Superconductivity in epitaxially grown $LaVO_3/KTaO_3(111)$ heterostructures

Yuan Liu(刘源)[1,†], Zhongran Liu(刘中然)[2,†], Meng Zhang(张蒙)[1], Yanqiu Sun(孙艳秋)[1], He Tian(田鹤)[2,3], and Yanwu Xie(谢燕武)[1,4,‡]

[1] *Interdisciplinary Center for Quantum Information, State Key Laboratory of Modern Optical Instrumentation, and Zhejiang Province Key Laboratory of Quantum Technology and Device, School of Physics, Zhejiang University, Hangzhou* 310027, *China*

[2] *Center of Electron Microscope, State Key Laboratory of Silicon Materials, School of Materials Science and Engineering, Zhejiang University, Hangzhou* 310027, *China*

[3] *School of Physics and Microelectronics, Zhengzhou University, Zhengzhou* 450052, *China*

[4] *Collaborative Innovation Center of Advanced Microstructures, Nanjing University, Nanjing* 210093, *China*

(Received 7 November 2022; revised manuscript received 7 December 2022; accepted manuscript online 16 December 2022)

Complex oxide heterointerfaces can host a rich of emergent phenomena, and epitaxial growth is usually at the heart of forming these interfaces. Recently, a strong crystalline-orientation-dependent two-dimensional superconductivity was discovered at interfaces between $KTaO_3$ single-crystal substrates and films of other oxides. Unexpectedly, rare of these oxide films was epitaxially grown. Here, we report the existence of superconductivity in epitaxially grown $LaVO_3/KTaO_3(111)$ heterostructures, with a superconducting transition temperature of ~ 0.5 K. Meanwhile, no superconductivity was detected in the (001)- and (110)-orientated $LaVO_3/KTaO_3$ heterostructures down to 50 mK. Moreover, we find that for the $LaVO_3/KTaO_3(111)$ interfaces to be conducting, an oxygen-deficient growth environment and a minimum $LaVO_3$ thickness of ~ 0.8 nm (~ 2 unit cells) are needed.

Keywords: interfaces, superconductivity, epitaxy

PACS: 73.40.–c, 74.25.F–, 81.15.–z

DOI: 10.1088/1674-1056/acac1b

1. Introduction

With the development of advanced film fabrication technology, nowadays it has been routine to grow high-quality epitaxial films for many materials. This is particularly true for complex oxides,[1–3] a big class of versatile materials that exhibit a wide range of exciting properties including superconductivity, ferromagnetism, ferroelectricity and many others. The ability to grow complex oxides epitaxially upon each other has led to many interfaces that host novel emergent phenomena.[1–3] Good examples include the $LaAlO_3/SrTiO_3$ interface that shows high-mobility electron gas,[4] 2D superconductivity,[5,6] and unusual magnetism,[7–9] the high-temperature superconducting bilayers of copper oxides,[10–12] and the $PbTiO_3/SrTiO_3$ superlattices with polar vortices.[13] Recently, an unusual 2D superconductivity was found at interfaces between $KTaO_3$ single-crystal substrates and other oxide films.[14–22] Unexpectedly, rare of these films is epitaxial: EuO is polycrystalline,[15,16] and $LaAlO_3$,[15,17–20] $YAlO_3$,[21] and TiO_x[22] are amorphous. Therefore, the role of epitaxial growth in the $KTaO_3$ interface superconductivity is still elusive.

$LaVO_3$ is a Mott–Hubbard insulator.[23,24] Previous studies[25,26] showed that it can be grown epitaxially on $KTaO_3(001)$ and forms a conducting interface. In this work, we grow epitaxial $LaVO_3$ thin films on all the (001)-, (110)-, and (111)-oriented $KTaO_3$ substrates and study their transport properties. We find that while all these $LaVO_3/KTaO_3$ interfaces can be conducting, only the (111)-interface is superconducting. However, the superconducting transition temperature T_c is much lower than the corresponding values in the previous non-epitaxial interfaces.[15–22] In addition, we find that, for the $LaVO_3/KTaO_3(111)$ interfaces to be conducting, an oxygen-deficient growth environment and a minimum $LaVO_3$ thickness of ~ 0.8 nm (~ 2 unit cells) are needed. Together with other control experiments, it suggests that electron transfer from oxygen vacancies in $LaVO_3$ film to $KTaO_3$ substrate is responsible for the interface conduction.

2. Experiment methods

$KTaO_3$ is a band insulator that has a cubic perovskite structure with a lattice constant of 0.3989 nm.[27] $LaVO_3$ has a $GdFeO_3$-type orthorhombic structure with lattice parameters of $a = 0.5555$ nm, $b = 0.7849$ nm, and $c = 0.5553$ nm at room temperature.[23,24] This structure can be regarded as a pseudocubic subcell with a lattice parameter $a_p \approx a/\sqrt{2} \approx b/2 \approx c/\sqrt{2} \approx 0.3926$ nm. The $LaVO_3$ thin films were grown in a high vacuum pulsed laser deposition chamber with a base pressure of $\sim 4 \times 10^{-8}$ mbar. The (001)-, (110)-, and (111)-

[†]These authors contributed equally to this work.

[‡]Corresponding author. E-mail: ywxie@zju.edu.cn

© 2023 Chinese Physical Society and IOP Publishing Ltd

oriented $KTaO_3$ single-crystal substrates were purchased from Hefei Kejing Materials Technology Co. Ltd. A $LaVO_4$ ceramic target was ablated with a pulsed KrF excimer laser ($\lambda = 248$ nm). Repetition rate of laser was 2 Hz and fluence at the target surface was ~ 3 J/cm^2. The growth temperature was 750 °C. If not specified, the growth was performed at $P(O_2) = 0$ mbar. The film thickness was controlled by counting the growth laser pulses after calibrating the growth rate by small-angle x-ray reflectivity measurement (Fig. S2). After growth, the samples were cooled down to room temperature with 50 °C/min under the growth atmosphere.

The atomic force microscopy data were taken on a Park NX10 system using noncontact mode. X-ray diffraction data were taken on a 3-kW high-resolution Rigaku Smart Lab system. Cross-sectional specimens for electron microscopy investigations were prepared by a FEI Quanta 3D FEG focused ion beam. Scanning transmission electron microscopy (STEM) images and energy-dispersive x-ray spectroscopy (EDS) mappings were acquired using a spherical aberration-corrected microscope equipped with four Super-X EDS detectors (FEI Titan G2 80-200 Chemi STEM, 30 mrad convergence angle).

The contacts to the $LaVO_3/KTaO_3$ interfaces of transport measurements were made by ultrasonic bonding with Al wires. DC transport measurements were carried out in a commercial physical property measurement system (PPMS, Quantum Design) with a dilution refrigerator insert and in a commercial ^{4}He cryostat with a ^{3}He insert (Cryogenic Ltd.) with a standard four-probe method.

3. Results

3.1. Structural characterizations

Atomic force microscopy images show that the surfaces of all the films are flat, with a root mean square roughness less than 0.4 nm (Fig. S1). From the fitting of small-angle x-ray reflectivity measurement, we can simulate that the interface and surface roughness is about 0.1 nm and 0.37 nm, respectively, indicating the high quality of the heterostructures. Figure 1(a) shows the x-ray diffraction (XRD) θ–2θ scan of a typical $LaVO_3/KTaO_3(111)$ sample. A clear and sharp $LaVO_3(111)$ peak was observed, which indicates that the film is single-phase and epitaxially oriented. From the position of the (111) diffraction peak of the film, the c-axis lattice constant d_{111} is found to be 0.226 nm ($\sqrt{3}d_{111} = 0.392$ nm) — is nearly the same as that in bulk $LaVO_3$.[23] Figure 1(b) shows a reciprocal space mapping (RSM) around the (132) perovskite peak. The vertical alignment of the film and substrate peaks indicates that the film is fully strained to the substrate. The crystalline quality of the $LaVO_3/KTaO_3(111)$ sample was further examined by out-of-plane ω-scan rocking curve. The full width at half maximum (FWHM) is only about 0.09° (Fig. 1(c)). These observations suggest that the $LaVO_3$ film is epitaxially grown on the $KTaO_3(111)$ substrate. Similar θ–2θ scans and RSM images were found for the $LaVO_3/KTaO_3(001)$ and $LaVO_3/KTaO_3(110)$ samples (Figs. S3 and S4), indicating that the growths were epitaxial in all of them.

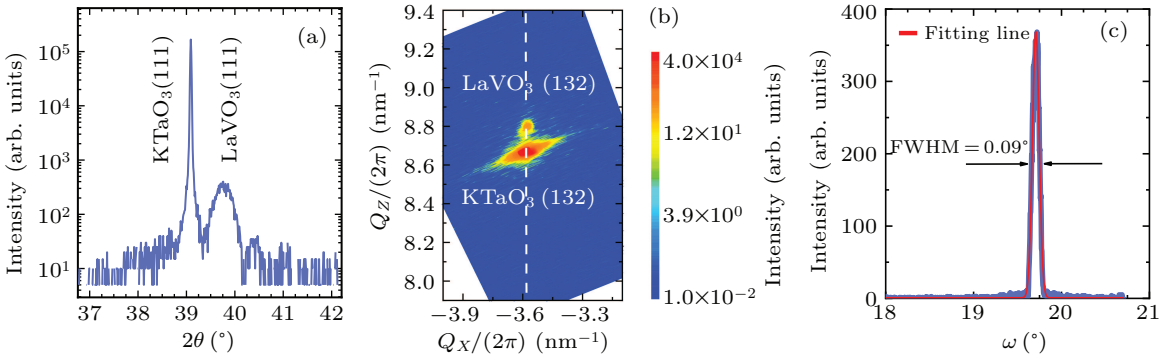


Fig. 1. X-ray diffraction of a $LaVO_3$(17 nm)/$KTaO_3$(111) heterostructure. (a) Out-of-plane θ–2θ XRD pattern. (b) Reciprocal space mapping around the (132) reflection. $LaVO_3$ and $KTaO_3$ Bragg's peaks aligned along the vertical dashed line. (c) Rocking curve taken of the $LaVO_3$ film.

The epitaxial growth of $LaVO_3$ on $KTaO_3$ is further evidenced by STEM measurements. In Figs. 2(a) and 2(b), we present STEM high-angle annular dark-field (HAADF) images taken from a $LaVO_3$(17 nm)/$KTaO_3$(111) sample. One can see that the $LaVO_3$ film is coherently and epitaxially grown on the $KTaO_3(111)$ substrate. Note that the smeared brightness ($\sim$ 1–2 nm wide) along the interface is caused by interface diffusion. In our STEM-HAADF images, the visible bright atomic spots are from La atoms in $LaVO_3$ and Ta atoms in $KTaO_3$. The interface diffusions of La–K and V–Ta add extra brightness in $KTaO_3$ and $LaVO_3$ sides, respectively, which result in the smeared brightness. EDS elemental mappings (Figs. 2(c)–2(f)) show that the interface diffusion is moderate, and the depth of the diffused region in each side is limited to within 1 nm from the interface. This value is much smaller than the thickness of the interface superconducting (conducting) channel.[14,18,21]

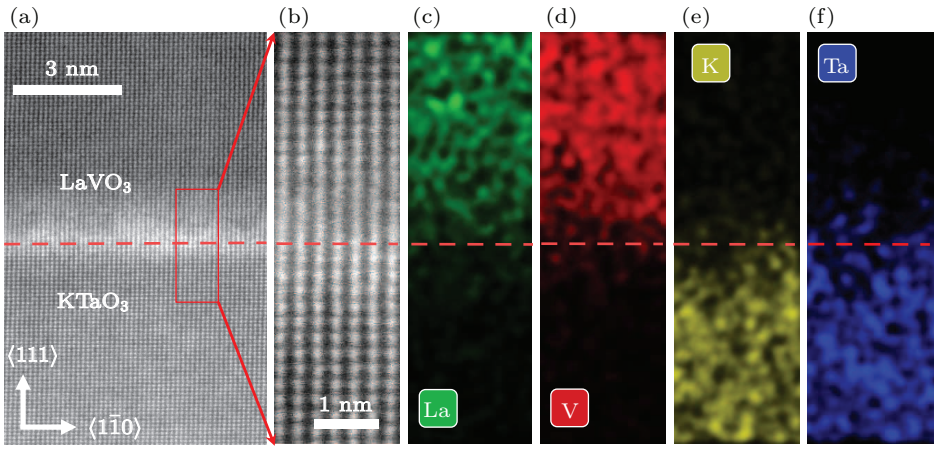


Fig. 2. STEM characterization of a $LaVO_3$(17 nm)/$KTaO_3$(111) heterostructure. (a), (b) HAADF-STEM images show that the $LaVO_3$ film is epitaxially grown on $KTaO_3$. (c)–(f) EDS elemental mappings of the same sample. A moderate interface diffusion is observed but the depth of the diffused region is within 1 nm in each side.

3.2. Transport properties

Figure 3(a) shows the temperature dependence of sheet resistance $R_{\rm sheet}$ for $LaVO_3$/$KTaO_3$ heterostructures. An overall metallic conduction is observed on all of them. At a given temperature, $R_{\rm sheet}$ decreases in a sequence following (111), (110) and (001), which is similar to that observed in previous amorphous-$LaAlO_3$/$KTaO_3$ heterostructures[17] and ionic-liquid-gated $KTaO_3$ surfaces.[28] Control experiments on $LaVO_3$ films grown on insulating $(La_{0.3}Sr_{0.7})(Al_{0.65}Ta_{0.35})O_3$ and $NdGaO_3$ substrates (see Figs. S5 and S6) demonstrate that the $LaVO_3$ films themselves are insulating, with $R_{\rm sheet}$ values several orders of magnitude higher than that of the present $LaVO_3$/$KTaO_3$ heterostructures. Therefore, the observed conduction can be solely ascribed to the conducting $LaVO_3$/$KTaO_3$ interfaces.

As shown in Fig. 3(b), a superconducting state with a mid-point T_c of 0.51 K is observed in the $R_{\rm sheet}(T)$ curve of the (111) sample, which is much lower than T_c ($\sim$ 2 K) of $LaAlO_3$/$KTaO_3$(111).[18] In contrast, no superconducting transition is detected in the (001) and (110) samples down to 50 mK. The normal-state magnetic-field-dependent Hall resistance measured at 2 K (Fig. 3(c)) on the (111) sample shows that the charge carriers are electrons, and the carrier density $n_{\rm sheet}$ and Hall mobility $\mu_{\rm Hall}$ are $\sim 1.4\times10^{14}$ cm^{-2} and ~ 42 cm$^2\cdot$V$^{-1}\cdot$s^{-1}, respectively. Similarly, the measured $n_{\rm sheet}$ and $\mu_{\rm Hall}$ for the (001) and (110) samples are $\sim 1.6\times10^{14}$ cm^{-2} and ~ 340 cm$^2\cdot$V$^{-1}\cdot$s^{-1}, and $\sim 1.1\times10^{14}$ cm^{-2} and $\sim$ 169 cm$^2\cdot$V$^{-1}\cdot$s^{-1}, respectively. These values are comparable with those of the corresponding $LaAlO_3$/$KTaO_3$ interfaces.[17,18]

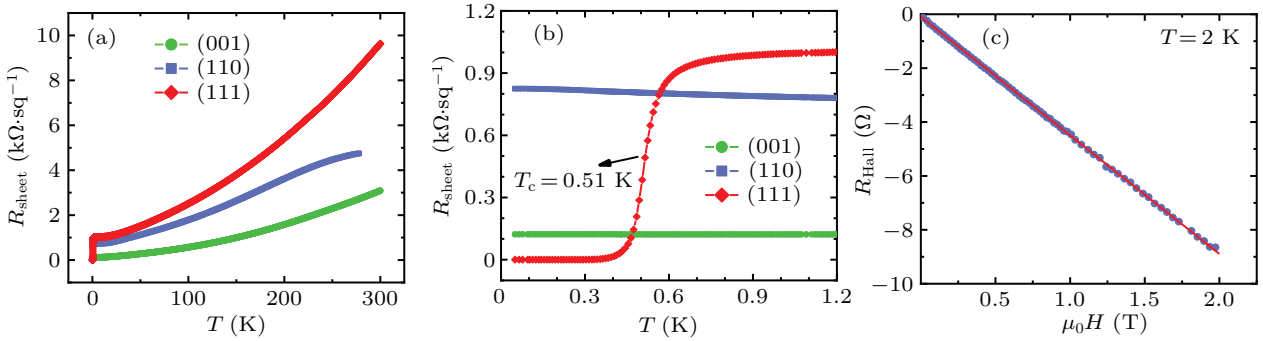


Fig. 3. Transport properties of epitaxial $LaVO_3$(17 nm)/$KTaO_3$ heterostructures. (a) Temperature-dependent $R_{\rm sheet}(T)$ curves from 300 K to 50 mK. (b) An enlarged view of the low-temperature data shown in (a). (c) Hall resistance $R_{\rm Hall}$ as a function of out-of-plane magnetic field for the (111) sample measured at 2 K.

3.3. Magnetoresistance

The superconducting state of $LaVO_3$/$KTaO_3$(111) is further studied by magnetoresistance measurements. Figures 4(a) and 4(b) display temperature-dependent $R_{\rm sheet}(T)$ values for magnetic fields applied perpendicular and parallel to the interface, respectively. The T_c can be completely suppressed by application of a perpendicular (or parallel) field $\mu_0 H = 0.2$ T (or 2 T) (here μ_0 is the vacuum permeability). Figures 4(c) and 4(d) display the temperature-dependent upper critical field μH_{c2}, derived from the $R_{\rm sheet}(T)$ curves shown in Figs. 4(a) and 4(b). The temperature dependences of both $\mu H_{c2}^{\perp}$ and $\mu H_{c2}^{\parallel}$ show a linear behavior, which is different from the 2D Ginzburg–Landau model and may indicate a 3D anisotropic superconductor behavior.[29–31] We suppose that a wider superconducting thickness leads to the phenomenon.

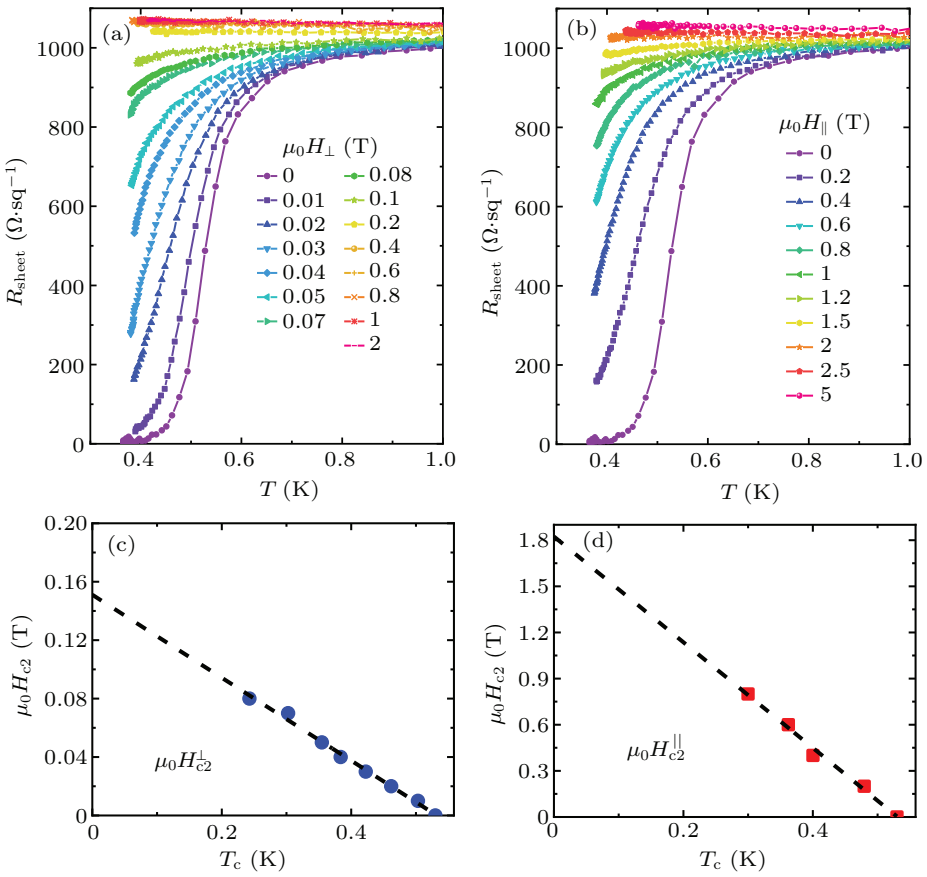


Fig. 4. Transport behaviors under magnetic field for the $LaVO_3$(17 nm)/$KTaO_3$(111) heterostructure. Dependence of $R_{\rm sheet}$ on T for a field (a) perpendicular and (b) parallel to the interface. Temperature dependence of upper critical field $\mu_0 H_{c2}$, extracted from the 50% normal-state resistance, (c) perpendicular and (d) parallel to the interface.

3.4. Oxygen vacancies and critical thickness

As far as the interface conduction is concerned, we find that the oxygen pressure $P(O_2)$ during growth and the thickness of $LaVO_3$, $d_{\rm LVO}$, are crucial. In Fig. 5(a) we display the $R_{\rm sheet}(T)$ curves for $LaVO_3/KTaO_3$(111) heterostructures grown at different $P(O_2)$ values. The interfaces are highly insulating when the heterostructures were grown at $P(O_2) = 10^{-5}$ mbar and above, and metallic (superconducting) when grown at $P(O_2) = 10^{-6}$ mbar and below. This suggests strongly that oxygen vacancies play a determinant role in the interface conduction. Moreover, we find that while the heterostructure grown at $P(O_2) = 0$ mbar is superconducting, the one grown at $P(O_2) = 10^{-6}$ mbar is metallic but not superconducting. In addition, for the interfaces to be conducting, $d_{\rm LVO}$ has to reach a critical thickness $d_c \sim 0.8$ nm. Note that this d_c value is much smaller than that of $LaAlO_3/KTaO_3$(111), ~ 3 nm. As shown in Fig. 5(b), the sheet conductance σ_s of the $LaVO_3/KTaO_3$(111) interface is below the measurement limit for $d_{\rm LVO} < 0.8$ nm, and reaches saturation in an order of 10^{-4} Ω^{-1} for $d_{\rm LVO} > 2$ nm. For a $d_{\rm LVO}$ between 0.8 nm and 2 nm, the corresponding σ_s can be large initially but decay severely with time in days (Fig. 5(c)).

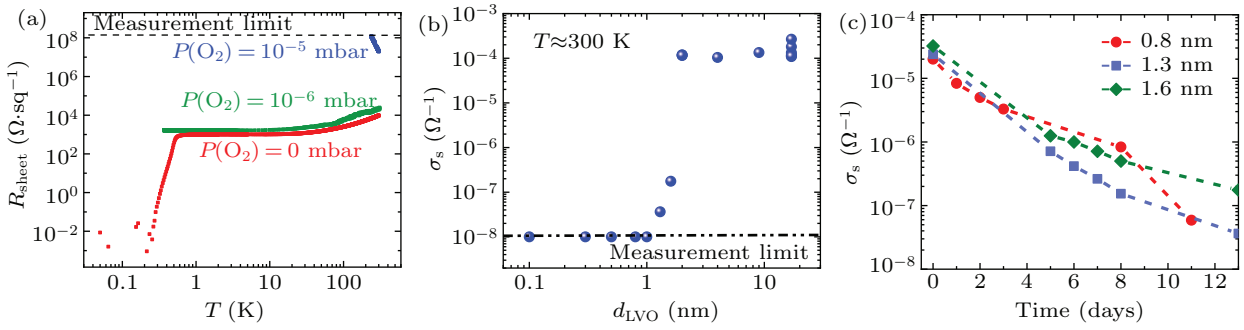


Fig. 5. Effects of growth oxygen pressure and $LaVO_3$ thickness. (a) $R_{\rm sheet}(T)$ curves for $LaVO_3$(17 nm)/$KTaO_3$(111) heterostructures grown under different oxgyen environments. (b) Room-temperature conductance σ_s of $LaVO_3/KTaO_3$(111) heterostructures grown at $P(O_2) = 0$ mbar for different $d_{\rm LVO}$ values. The data were measured after the conductance became stable. (c) Decay of σ_s with time for $LaVO_3/KTaO_3$(111) heterostuctures of small $d_{\rm LVO}$.

4. Discussion

First, we discuss the conduction mechanism of the epitaxial $LaVO_3/KTaO_3$ heterostructures. Previously we have demonstrated that the interface conduction in $LaAlO_3/KTaO_3$ heterostructures is controlled by electron transfer from oxygen vacancies in $LaAlO_3$ film to $KTaO_3$ substrate near the interface.[19] Here we propose that the same mechanism, that is, electron transfer from oxygen vacancies in $LaVO_3$ to $KTaO_3$, applies for the $LaVO_3/KTaO_3$ heterostructures. This scenario is supported by that a low $P(O_2)$, which can induce oxygen vacancies in $LaVO_3$, is necessary for the creation of interface conduction (Fig. 5(a)). It is further supported by that the interface conduction exhibits a gradual decay with time when d_{LVO} is small, which can be explained by a gradual refilling of oxygen vacancies in $LaVO_3$ from ambient oxygen sources. Furthermore, note that although a low $P(O_2)$ can also induce oxygen vacancies in $KTaO_3$, we exclude them as a determinant conduction origin because even with them, the $LaVO_3/KTaO_3$ interface is still insulating if $d_{LVO} < d_c$ (including the bare KTO) (Fig. 5(b)). In $LaAlO_3/SrTiO_3$, after a long-standing debate,[32–37] one widely accepted viewpoint[38] is that the key role of interface polar discontinuity is to form thermodynamically stable oxygen vacancies at the surface of $LaAlO_3$,[38] which eventually transfer electrons to the interface. Therefore, the oxygen-vacancies-induced electron transfer and the classical electronic reconstruction share similar feature — electron transfer from oxygen vacancies in the film to the interface.[38–40] The key difference lies in the formation mechanism of oxygen vacancies. In $LaVO_3/KTaO_3$, it is reasonable to argue that the oxygen-deficient growth atmosphere, rather than the polar issue, is the main source of oxygen vacancies in $LaVO_3$.

Next, we discuss the superconductivity observed in the present epitaxial $LaVO_3/KTaO_3(111)$ heterostructures. In the non-epitaxial $EuO/KTaO_3$ and $LaAlO_3/KTaO_3$ heterostructures, superconductivity was found at the (111) ($T_c \sim 2$ K)[15,18] and (110) ($T_c \sim 0.9$ K)[17] interfaces, but absent at the (001) interfaces.[15,17] A superconductivity of similar properties was also achieved on the bare $KTaO_3$ surfaces using an ionic liquid gating.[28] These results suggest that the $KTaO_3$ interface superconductivity is determined by the intrinsic properties of electron-doped surfaces of $KTaO_3$. Thus one would expect a superconductivity of similar properties in $LaVO_3/KTaO_3$ heterostructures. However, as shown in Fig. 3, only $LaVO_3/KTaO_3(111)$ is superconducting, and its T_c is much lower compared with that of the non-epitaxial ones (~ 0.5 K vs. ~ 2 K). We speculate that the weaker superconductivity in $LaVO_3/KTaO_3(111)$ is related to a wider conducting channel than that in the previous non-epitaxial ones.

5. Summary

In summary, we have fabricated epitaxial $LaVO_3$ film on $KTaO_3$ substrate and shown that a $T_c \sim 0.5$ K superconductivity can be obtained in epitaxially grown $LaVO_3/KTaO_3(111)$ heterostructure. By contrast, no superconductivity is detected down to 50 mK in the epitaxially grown $LaVO_3/KTaO_3(001)$ and $LaVO_3/KTaO_3(110)$ heterostructures. Although in an earlier study,[28] we have demonstrated that the presence of an oxide interface is not a prerequisite for the occurrence of $KTaO_3$ interface superconductivity, our present result, together with these previous ones,[14–22] demonstrates that the detailed condition of an oxide interface still plays an important role in determining the superconductivity.

Acknowledgements

Project supported by the National Natural Science Foundation of China (Grant Nos. 11934016 and 12074334), the Key R&D Program of Zhejiang Province, China (Grant Nos. 2020C01019 and 2021C01002), and the Fundamental Research Funds for the Central Universities of China.

Y.L., M.Z. and Y.S. fabricated and characterized the heterostructures. Z.L. and H.T. measured and analyzed the STEM data. Y.L. and Y.X. wrote the manuscript with input from all authors.

References

[1] Hwang H Y, Iwasa Y, Kawasaki M, Keimer B, Nagaosa N and Tokura Y 2012 *Nat. Mater.* **11** 103
[2] Lorenz M, Ramachandra Rao M S, *et al.* 2016 *J. Phys. D. Appl. Phys.* **49** 433001
[3] Liu X, Middey S, Cao Y, Kareev M and Chakhalian J 2016 *MRS Commun.* **6** 133
[4] Ohtomo A and Hwang H Y 2004 *Nature* **427** 423
[5] Reyren N, Thiel S, Caviglia A D, Fitting Kourkoutis L, Hammerl G, Richter C, Schneider C W, Kopp T, Rüetschi A S, Jaccard D, Gabay M, Muller D A, Triscone J M and Mannhart J 2007 *Science* **317** 1196
[6] Caviglia A D, Gariglio S, Reyren N, Jaccard D, Schneider T, Gabay M, Thiel S, Hammerl G, Mannhart J and Triscone J M 2008 *Nature* **456** 624
[7] Brinkman A, Huijben M, Van Zalk M, Huijben J, Zeitler U, Maan J C, Van Der Wiel W G, Rijnders G, Blank D H A and Hilgenkamp H 2007 *Nat. Mater.* **6** 493
[8] Li L, Richter C, Mannhart J and Ashoori R C 2011 *Nat. Phys.* **7** 762
[9] Bert J A, Kalisky B, Bell C, Kim M, Hikita Y, Hwang H Y and Moler K A 2011 *Nat. Phys.* **7** 767
[10] Gozar A, Logvenov G, Kourkoutis L F, Bollinger A T, Giannuzzi L A, Muller D A and Bozovic I 2008 *Nature* **455** 782
[11] Deng J, Ren T, Ju L, Zhang H, Sun J, Shen B and Xie Y 2020 *Sci. China Mater.* **63** 128
[12] Ju L, Ren T, Li Z, Liu Z, Shi C, Liu Y, Hong S, Wu J, Tian H, Zhou Y and Xie Y 2022 *Phys. Rev. B* **105** 024516
[13] Yadav A K, Nelson C T, Hsu S L, Hong Z, Clarkson J D, Schlepuëtz C M, Damodaran A R, Shafer P, Arenholz E, Dedon L R, Chen D, Vishwanath A, Minor A M, Chen L Q, Scott J F, Martin L W and Ramesh R 2016 *Nature* **530** 198
[14] Hua X, Meng F, Huang Z, Li Z, Wang S, Ge B, Xiang Z and Chen X 2022 *npj Quantum Mater.* **7** 97
[15] Liu C, Yan X, Jin D, Ma Y, Hsiao H W, Lin Y, Bretz-Sullivan T M, Zhou X, Pearson J, Fisher B, Jiang J S, Han W, Zuo J M, Wen J, Fong D D, Sun J, Zhou H and Bhattacharya A 2021 *Science* **371** 716
[16] Ma Y, Niu J, Xing W, Yao Y, Cai R, Sun J, Xie X C, Lin X and Han W 2020 *Chin. Phys. Lett.* **37** 117401

[17] Chen Z, Liu Z, Sun Y, Chen X, Liu Y, Zhang H, Li H, Zhang M, Hong S, Ren T, Zhang C, Tian H, Zhou Y, Sun J and Xie Y 2021 *Phys. Rev. Lett.* **126** 26802

[18] Chen Z, Liu Y, Zhang H, Liu Z, Tian H, Sun Y, Zhang M, Zhou Y, Sun J and Xie Y 2021 *Science* **372** 721

[19] Sun Y, Liu Y, Hong S, Chen Z, Zhang M and Xie Y 2021 *Phys. Rev. Lett.* **127** 086804

[20] Sun Y, Liu Y, Pan W and Xie Y 2022 *J. Phys.: Condens. Matter* **34** 444004

[21] Zhang G, Wang L, Wang J, Huang G, Yang G, Xue H, Wu Y, Xu J, Song Y, An Z, Zheng C, Shen J, Li J, Chen Y and Li W 2021 *arXiv:2111.05650v5*

[22] Al-Tawhid A H, Kanter J, Hatefipour M, Kumah D P, Shabani J and Ahadi K 2022 *J. Electron. Mater.* **51** 6305

[23] Bordet P, Chaillout C, Marezio M, Huang Q, Santoro A, Cheong S W, Takagi H, Oglesby C S and Batlogg B 1993 *J. Solid State Chem.* **106** 253

[24] Jana A, Choudhary R J and Phase D M 2018 *Phys. Rev. B* **98** 075124

[25] Wadehra N, Tomar R, Varma R M, Gopal R K, Singh Y, Dattagupta S and Chakraverty S 2020 *Nat. Commun.* **11** 874

[26] Goyal S, Wadehra N and Chakraverty S 2020 *Adv. Mater. Interfaces* **7** 2000646

[27] Wemple S H 1965 *Phys. Rev.* **137** A1575

[28] Ren T, Li M, Sun X, Ju L, Liu Y, Hong S, Sun Y, Tao Q, Zhou Y, Xu Z A and Xie Y 2022 *Sci. Adv.* **8** eabn4273

[29] Tinkham M 2004 *Introduction to Superconductivity* (Courier Corporation) p. 324

[30] Ruggiero S T, Barbee T W and Beasley M R 1980 *Phys. Rev. Lett.* **45** 1299

[31] Nakagawa Y, Saito Y, Nojima T, Inumaru K, Yamanaka S, Kasahara Y and Iwasa Y 2018 *Phys. Rev. B* **98** 064512

[32] Nakagawa N, Hwang H Y and Muller D A 2006 *Nat. Mater.* **5** 204

[33] Liu Z Q, Li C J, Lü W M, Huang X H, Huang Z, Zeng S W, Qiu X P, Huang L S, Annadi A, Chen J S, Coey J M D, Venkatesan T and Ariando 2013 *Phys. Rev. X* **3** 021010

[34] Siemons W, Koster G, Yamamoto H, Harrison W A, Lucovsky G, Geballe T H, Blank D H A and Beasley M R 2007 *Phys. Rev. Lett.* **98** 196802

[35] Reinle-Schmitt M L, Cancellieri C, Li D, Fontaine D, Medarde M, Pomjakushina E, Schneider C W, Gariglio S, Ghosez P, Triscone J M and Willmott P R 2012 *Nat. Commun.* **3** 932

[36] Zhang M, Chen Z, Mao B, Li Q, Bo H, Ren T, He P, Liu Z and Xie Y 2018 *Phys. Rev. Mater.* **2** 065002

[37] Zhang M, Du K, Ren T, Tian H, Zhang Z, Hwang H Y and Xie Y 2019 *Nat. Commun.* **10** 4026

[38] Yu L and Zunger A 2014 *Nat. Commun.* **5** 5118

[39] Chen Z, Chen X, Mao B, Li Q, Zhang M, Bo H, Liu Z, Tian H, Zhang Z and Xie Y 2018 *Adv. Mater. Interfaces* **5** 1801216

[40] Chen Z, Zhang M, Ren T and Xie Y 2019 *J. Phys.: Condens. Matter* **31** 505002